Microstructure evolution in density relaxation by tapping

Anthony D. Rosato,[1] Oleksandr Dybenko,[1] David J. Horntrop,[2] Vishagan Ratnaswamy,[1] and Lou Kondic[2]
[1]*Granular Science Laboratory, Department of Mechanical and Industrial Engineering, New Jersey Institute of Technology, Newark, New Jersey 07102, USA*
[2]*Department of Mathematical Sciences and Center for Applied Mathematics and Statistics, New Jersey Institute of Technology, Newark, New Jersey 07102, USA*

(Received 30 August 2009; revised manuscript received 13 January 2010; published 8 June 2010)

The density relaxation phenomenon is modeled using both Monte Carlo and discrete element simulations to investigate the effects of regular taps applied to a vessel having a planar floor filled with monodisperse spheres. Results suggest the existence of a critical tap intensity which produces a maximum bulk solids fraction. We find that the mechanism responsible for the relaxation phenomenon is an evolving ordered packing structure propagating upwards from the plane floor.

DOI: 10.1103/PhysRevE.81.061301 PACS number(s): 45.70.−n, 05.65.+b, 02.70.Ns, 81.05.Rm

I. INTRODUCTION

Density relaxation describes the phenomenon in which granular solids undergo an increase in bulk density as a result of properly applied external loads. The ability of granular materials to undergo density changes is an inherent property that is not well-understood, and thus it remains a critical impediment in developing predictive models of flowing bulk solids. From a historical perspective, studies on density relaxation have their basis in the extensive literature on the packing of particles [1], where the concern was often in characterizing loose and dense random structures.

The focus of early studies on density relaxation was on how optimal packings could be produced through the use of continuous vibrations or discrete taps [2–4]. Recently, there has been a resurgence of interest (partly triggered by experiments [5–8]) in uncovering particle-level mechanisms responsible for observed macroscopic behavior. These experimental results have spurred theoretical studies involving free volume arguments [9], parking lot paradigms [10–13], and stroboscopic decay approaches [14,15]. Computational investigations involving stochastic and deterministic simulations [16–23] have also been completed to directly address the coupling between the detailed particle dynamics and bulk behavior. In this regard, we note the single particle and collective dynamics [17], the jump and push filling mechanisms identified in [24], and the appearance of local structural order evidenced by a second peak in the radial distribution function [12]. The formation of an ordered structure was also discussed in [25], where it was shown that there is a narrow range of densities where disordered and crystalline structures are expected to coexist. The influence of shear and "crystallization by shear" was observed in experiments [26–28], while crystallization by horizontal shaking has been reported [29]. In addition, crystallization of cohesive and noncohesive particles was explored experimentally [30,31], where it was found that vibrational annealing can be successfully used to form almost perfect structures. Important progress related to density relaxation has also been made in characterizing glass and jamming transitions in granular materials [32].

The results reported in this paper provide significant insight regarding the process of density relaxation in granular materials exposed to discrete taps imposed by the motion of a flat plane floor. The process is modeled through (1) hard-sphere Monte Carlo (MC) simulations and (2) discrete element (DE) simulations using inelastic, frictional spheres. Although these particle-based methods are quite different (one purely stochastic and the other involving deterministic dynamics), both reveal a clear picture of the dynamical process responsible for density relaxation, namely, the upward progression of self-organized layers induced by the plane floor as the taps evolve. Indeed, its occurrence in both the MC and DE simulations suggests the universality of this mechanism in density relaxation which, to our knowledge, has not been previously reported in the literature. We also unambiguously demonstrate the importance of the nature of the applied tap in the temporal evolution of these granular systems. In particular, we highlight the essential difference in behavior when the system is subjected to continuous vibrations as opposed to discrete taps.

The remainder of this paper is organized as follows. We first describe our MC simulation model (reported in detail elsewhere [33]), which is based on a modification of the standard Metropolis scheme [34]. In this approach, the effect of taps applied to a containment vessel filled with spherical particles of diameter d is idealized by applying a normalized vertical lift $\Delta/d \equiv \gamma$ of the particle assembly from the floor. We demonstrate the importance of incorporating this separation (as compared to employing a uniform spatial expansion) to dislodge metastable configurations in attaining an increase in density. We find evidence of a critical tap intensity that optimizes the evolution of packing density. Next, we discuss our DE model and simulations, the results of which reveal the same tap-induced ordering effect of the floor on the local microstructure, provided that the amplitude and frequency of the tap are large enough.

II. MONTE CARLO SIMULATION MODEL

The computational domain used for the simulations in this paper is a box having a smooth flat floor and periodic boundary conditions in the lateral directions (x and z; $12d \times 12d$). These periodic conditions are used to eliminate the ordering effect of the side walls, as is commonly done. Spheres that

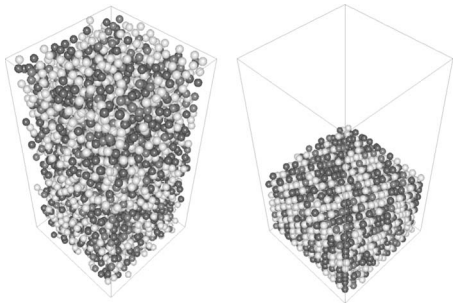

FIG. 1. Snapshot of a system of hard spheres within the periodic box for: (a) an initial, random state and (b) a configuration of the ensemble tapped at $\gamma=0.25$ for which $\langle\nu\rangle=0.6542$.

are at the outset randomly placed in the box, settle under gravity to a loose assembly, which will be termed a poured assembly. See Fig. 1(a) for a depiction of one such assembly. The poured assembly is then subjected to a series of taps of intensity γ. A typical assembly after the application of several taps is depicted in Fig. 1(b).

In our MC simulation, a single step in the algorithm consists of the random selection of a particle $\mathbf{x}_i=(x_i,y_i,z_i)$, followed by its assignment to a trial position $\mathbf{x}_i'=\mathbf{x}_i+\delta(1-2\xi)$, where ξ is a random vector with each component sampled from a uniform distribution on (0,1) and δ is the maximum allowed displacement. The trial position is accepted unconditionally (provided that an overlap does not occur) as the new location if the change in the system energy $\Delta E \equiv mg\Sigma_{i=1}^{N}(y_i'-y_i)\leq 0$. Otherwise, if the change in energy is positive ($\Delta E>0$), the trial position is accepted with probability $e^{-\beta\Delta E}$. For the macroscopic particles under study, β is set to a very large number ($\beta\equiv 1/kT$, where k is the Boltzmann constant) so that the likelihood of an accepted upward displacement is negligible. We remark that this choice of β yields the same results as directly precluding in the algorithm particle motions (i.e., $T=0$) that would yield an increase in the system energy. Another particle is then selected at random and the above procedure is repeated. As this settling process advances through many thousands of MC steps, the mean-free path decreases resulting in a drastically diminished rate of approach to a local equilibrium. Therefore, the parameter δ is modified every 10^4 MC steps in accordance to $\delta'=0.995\delta$ if fewer than half of these steps are accepted.

The effect of a single tap applied to a containment vessel filled with spherical particles of diameter d is idealized by lifting the entire particle assembly from the floor by an amount Δ, whose normalized value is $\gamma\equiv\Delta/d$. Our assumption here is that a tap is sufficiently energetic to cause a small separation of the assembly from the floor. That is, γ physically represents the lift that a granular mass will experience as it is energetically tapped. Within a single tap n of intensity γ, we monitored the bulk solids fraction $\nu_j(n;\gamma)$ (i.e., the fraction of volume occupied by spheres) at MC step j every 10^6 steps. The settling process was terminated when the difference in bulk solids fractions $|\nu_{(k+1)10^6}(n;\gamma)-\nu_{10^6k}(n;\gamma)|<0.001$, $k=0,1,2,\ldots$ This protocol was validated by enforcing the latter criterion twice to ensure that premature termination could not occur.

The Monte Carlo approach used here is essentially akin to the energy landscape ideas introduced by Luding *et al.* [35] and applied in [36]. In our simulations, the energy decreases until a local minimum is reached, at which point, the system is perturbed to move it out of this local minimum. The algorithm to accomplish this (akin to that used in [35]) is based on an acceptance probability $e^{-\beta\Delta E}$ (as described previously) where ΔE represents the change in system gravitational potential energy resulting from a random displacement of a particle. Thus, our MC approach seeks to find the minimum in potential energy corresponding to maximizing the bulk density.

Monte Carlo results

In all cases reported in this paper, poured assemblies consisting of 3 456 particles with solids fractions ν_o in the range 0.56 to 0.58 filled the periodic box to a depth of approximately $22d$. For each tap n, we computed the ensemble averaged bulk solids fraction $\langle\nu(n;\gamma)\rangle$ over M realizations, and its standard deviation $\langle\sigma(n;\gamma)\rangle=\sqrt{\frac{1}{M}\Sigma_{k=1}^{M}[\nu_k(n;\gamma)-\langle\nu(n;\gamma)\rangle]^2}$ where $\langle\nu(n;\gamma)\rangle=\frac{1}{M}\Sigma_{k=1}^{M}\nu_k(n;\gamma)$. The equilibrium bulk solids fraction $\nu_\infty(\gamma)$ was found by increasing the number of realizations over a sufficient number of taps N_T until the condition $\langle\sigma(N_T;\gamma)\rangle<0.001$ was satisfied.

Our MC tapping procedure differs from that used in [17], where vertical position-dependent displacements of the particles ($y'=\lambda y$) were applied in sync with random lateral perturbations. In an earlier paper [33], we reported that statistically equivalent solids fractions were obtained with or without application of these random lateral displacements. Furthermore, for the packings ($\sim 22d$ high) reported here, application of taps consisting of the vertical position-dependent displacements produced little or no increase in solids fraction in the upper portion of the bed [37], so that the bulk solids fraction remained relatively low. We attribute this behavior to an overly aggressive vertical displacement of the particles with distance from the floor, so that after each tap, the system tends to lose memory of its previous microstructure. Physically, this corresponds to the situation in which vigorous taps or shakes are applied so that the system relaxes to nearly the same or lower bulk density. We note that in addition to [37] results of this nature have also been recently reported in [23].

As further evidence of the importance of the choice of model for a tap in the Monte Carlo simulations, we considered two modes of tapping that produced the same increase in system potential energy. In the first, the particle assembly was lifted from the floor by an amount $\gamma=0.25$, while in the second tap mode, the system is dilated uniformly in the vertical direction, but particles that are initially touching the floor are not moved. This expansion mode is similar to a position-dependent vertical dilation of degree ε used in [38], where the dilated position $(y-d/2)'=(y-d/2)(1+\varepsilon)$, so that particles touching the floor are not allowed move upwards. Our MC results (Fig. 2) show that for the same increase in system potential energy due to the taps, a significantly higher densification rate occurred when the entire particle assembly was lifted as opposed to when the floor particles were held fixed. The ability to form of an ordered, densely packed layer

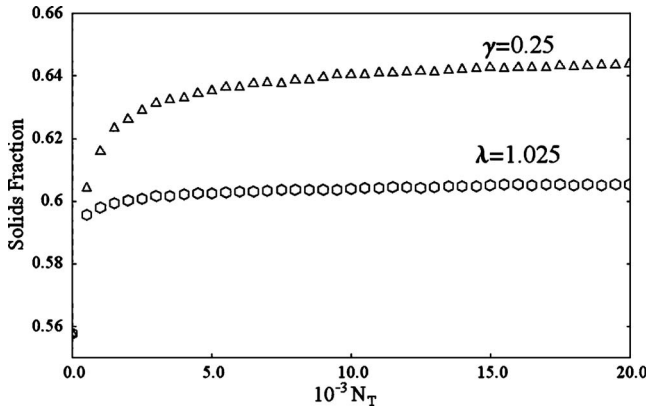

FIG. 2. Solids fraction versus tap number for two tap modes: $\gamma=0.25$ and $\lambda=1.025$, each producing the same increase in system potential energy.

of particles on the floor requires that these particles are also permitted to move upwards so that holes of sufficient size which open up in the first layer as the taps progress can readily be filled by particles above. The results of our MC simulations suggest that this mechanism plays a key role in microstructure formation throughout the system. Although not shown in this paper, extended studies carried out using the position-dependent dilation model revealed that little or no significant increase in bulk density could be attained even after the application of many thousands of taps. In what follows, the remainder of the MC results will employ the lift model ($\gamma \equiv \Delta/d$) for a tap. It is to be noted here that we are not suggesting that system dilation is unimportant, but rather that a separation from the floor is a critical feature in our MC simulations.

The simulated mean coordination number (i.e., average number of contacts per particle) versus solids fraction is shown in Fig. 3. In the calculation, particles i and j were deemed to be in contact when the distance between their centers $\|\mathbf{x}_i-\mathbf{x}_j\| \leq 1.05d$. The behavior of these simulation results is in reasonably good agreement with the experimental

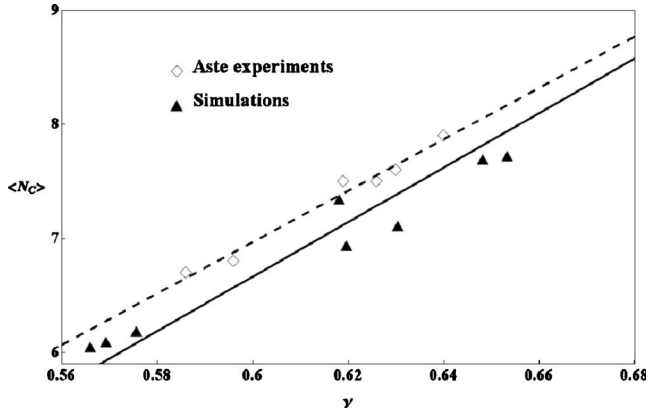

FIG. 3. Mean coordination number $\langle N_c \rangle$ versus solids fraction ν from the MC simulation (▲) and experimental measurements (◇) of Aste *et al.* [39]. The straight lines are linear regression fits to show the trends of experimental (dashed) and computational (solid) results.

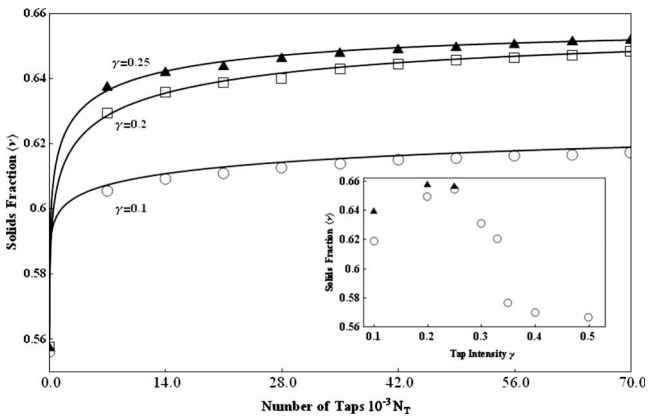

FIG. 4. Bulk solids fraction $\langle \nu \rangle$ versus the number of taps N_T at $\gamma=0.1,0.2,0.25$ (symbols) and fits (lines) to the KWW law $\nu(\eta) = \nu_\infty - (\nu_\infty - \nu_o)e^{-(\eta/\tau)^\beta}$. The inset shows $\langle \nu \rangle$ for $0.1 \leq \gamma \leq 0.5$. The solid triangles are the equilibrium solids fractions ν_∞ obtained from fit to the KWW law.

measurements of Aste *et al.* [39], showing the same trend over a range of ν. Since the error of the experimental results was not reported, we cannot comment on the significance of the slight shift of the two lines shown in Fig. 3. We found further corroboration (reported in [33]) of the simulation results in the fit of the solids fraction evolution data at low tap intensities to the inverse log phenomenological law reported in [5–8].

A series of case studies for $0.1 \leq \gamma \leq 0.5$ was carried out, from which the corresponding bulk solids fractions $\langle \nu \rangle$ were determined. Graphs of $\langle \nu \rangle$ versus the number of taps N_T for $\gamma=0.1,0.2,0.25$ are shown as the symbols in Fig. 4. For the purpose of clarity, graphs for larger values of γ were not included. We further analyzed the results for intensities $\gamma = 0.1,0.2,0.25$ by fitting the data to the Kohlrausch-Williams-Watts (KWW) law $\nu(n) = \nu_\infty - (\nu_\infty - \nu_o)e^{-(n/\tau)^\beta}$ as well as to extrapolate the equilibrium bulk solids fraction ν_∞. Corresponding to $\gamma=0.1,0.2,0.25$, the respective fit parameters were found to be $\tau=27180,1985,1083$ and $\beta = 0.2000,0.2588,0.2715$.

As it can be seen, the simulation data $\langle \nu \rangle$ conforms well with the fits to the KWW law (lines). The dependency of the densification rate on γ is shown on the inset of the figure; for $\gamma \geq 0.3$, equilibration was achieved quite rapidly requiring less than 10^4 taps. We were unable to run to equilibrium for $\gamma < 0.3$ because of the very large number of taps required. However, the equilibrium solids fractions ν_∞ from the fit to the KWW law (solid triangles) for $\gamma=0.1,0.2,0.25$ along with the data for $\gamma \geq 0.3$ reveal a nonmonotonic behavior that suggests the existence of a critical intensity which produces an optimal dense packing. This nonmonotonic behavior is in qualitative agreement with Fig. 2(a) of [40], where the stationary solids fraction versus dimensionless acceleration was plotted.

To further explore this hypothesis, the simulation process was reversed by starting with a hexagonal crystal structure ($\nu_o \cong 0.74$), which was subsequently tapped at the same intensities ($0.1 \leq \gamma \leq 0.5$) previously used. After only a few taps, the dense crystal structure is disrupted thereby causing

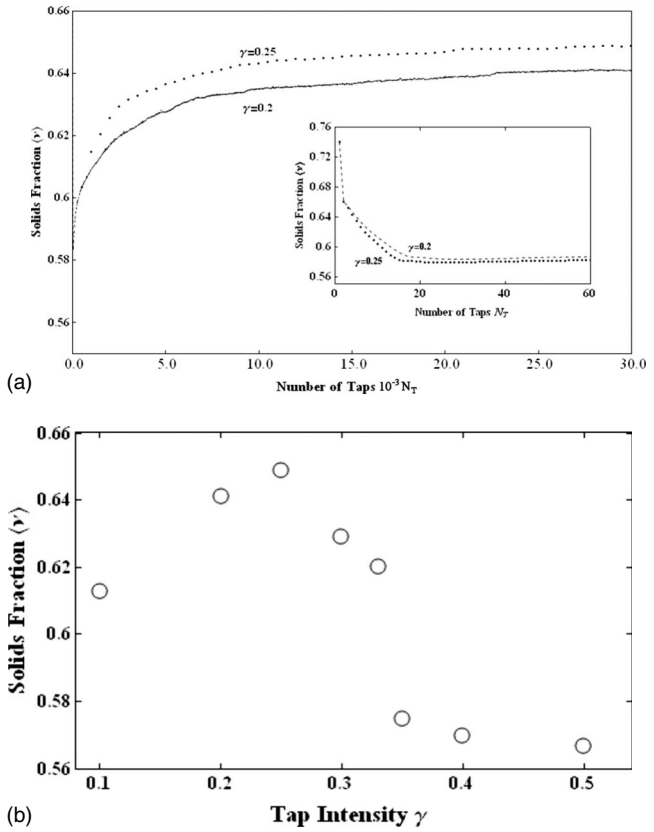

FIG. 5. Bulk solids fraction $\langle \nu \rangle$ versus the number of taps N_T at $\gamma=0.2,0.25$, for which the initial state was an hexagonal close-packed structure ($\nu_o=0.74$). The evolution of $\langle \nu \rangle$ for $0 \leq N_T \leq 60$ is shown in the inset (b). Graph of $\langle \nu \rangle$ versus tap intensity for $0.1 \leq \gamma \leq 0.5$.

a significant reduction in solids fraction; this can be seen during the first 60 taps as shown in the inset of Fig. 5(a). After many thousands of taps, the solids fraction graphs flatten as shown for intensity values $\gamma=0.20,0.25$ of Fig. 5(a). For large intensities, equilibration is attained for less than 10^4 taps. The results of this study are summarized in Fig. 5(b) and reveal a trend very similar to that observable in Fig. 4. That is, the graph peaks at roughly the same range of intensity values as in Fig. 4. This finding regarding the existence of a critical intensity is also supported by experiments reported elsewhere [37] and by the conjecture [41] that bulk density is related to impact velocity.

Figure 6 illustrates the mechanism responsible for density relaxation in our Monte Carlo model—namely, the upward advance of organized layers induced by the plane floor. The progression is quantified by the ensemble-averaged fraction of the total number of sphere centers $\bar{n}$ as function of the distance y/d from the floor. For the untapped poured system, $\bar{n}$ [Fig. 6(a)] is uniform except for a well-known ordering [42,43] of the first few layers adjacent to the floor. As the tapping proceeds, there is an upward advance of the layering: after 50 and 250 taps [Figs. 6(b) and 6(c))] peaks in $\bar{n}$ have formed near the floor, while at 90 000 taps [Fig. 6(d)], the peaks appear throughout the depth indicating organization present throughout the system. We remark that experimental evidence of the influence of a flat planar floor in promoting

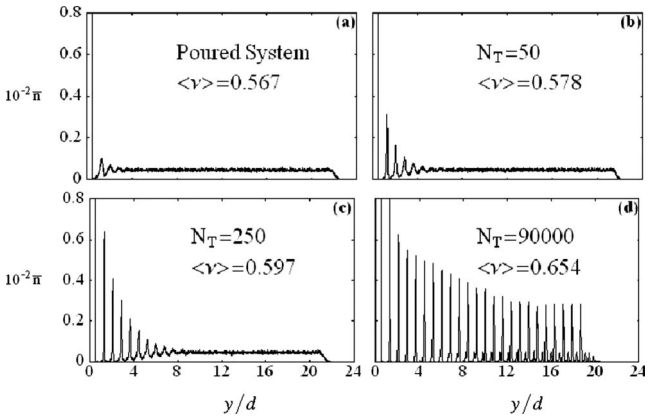

FIG. 6. MC ensemble-averaged fraction of the total number of sphere centers $\bar{n}$ as a function of y/d for tap intensity $\gamma=0.25$: (a) poured system, $\nu_o=0.567$; (b) 50 taps, $\langle \nu \rangle=0.578$; (c) 250 taps, $\langle \nu \rangle=0.597$; and (d) 90 000 taps, $\langle \nu \rangle=0.654$.

this ordering was reported in the Ref. [44]. Existence of mixed ordered/disordered regime in the similar density regime as considered here [0.64,0.66] was also discussed in [45].

A growth in the magnitude of the peaks as the taps evolve is a manifestation of a gradual structural reorganization and filling of voids. The increase from $\nu_o=0.567$ to $\langle \nu \rangle=0.654$ is accompanied by an (approximate) $2d$ reduction in the bed's effective height from its initial level. The locations of the peaks adjacent to the floor closely correspond to where they would be positioned in a hexagonal close-packed structure. As the number of taps increased, the number of peaks at which the correspondence held grew. In Fig. 6(d) one can also see smaller secondary peaks in the upper side of the bed, giving further evidence of (yet) an imperfect structure there. These secondary peaks gradually vanish as the ordering continues its propagation upwards through the assembly.

At this point, it is appropriate to comment on several earlier density relaxation studies reported in the literature, which are specifically relevant to the present investigation. In particular, results of experiments were reported [5,7,8] in which a tall cylindrical vessel (of approximately one meter in height and diameter D) filled with essentially monodisperse glass spheres was subject to sinusoidal pulses. Average solids fractions at three locations along the length of the cylinder were measured using a capacitance technique. From the data, a phenomenological law was extracted to describe the evolution of the solids fraction as a function of the number of taps n, given by $\nu(n)=\nu_\infty-\frac{\nu_\infty-\nu_o}{1+B\log(1+n/\tau)}$, where ν_o and ν_∞ are, respectively, the initial and equilibrium solids fractions, τ is a time scale, and B is a constant. As indicated earlier, we were able to fit our MC data to this functional form at lower tap intensity values, albeit our solids fraction values were higher than in the experiments. This discrepancy could be a result of wall affects due to the small aspect ratio used in the experiments ($D/d \sim 9.3$). We further note that since one of the objectives of these experiments was to describe the evolution of bulk density, attempts were not made to quantify the development of microstructure within the packing. Philippe and Bideau [40] reported on tapped cylinder experiments

$(D/d \sim 100)$ in which solids fraction data was fit to the KWW law to show a connection between compaction dynamics and "glassy" behavior. It is not clear if the authors examined microstructure evolution in the system. However, results from Ref. [44] do show evidence of ordering due to the presence of a flat floor.

While the results of our MC simulations are interesting in their own right, we also carry out discrete element simulations, which could be argued to be closer to a realistic physical system. As shown in the next section, the results of these studies exhibit the same qualitative behavior observed in the MC simulations, suggesting universality of the findings.

III. DISCRETE ELEMENT MODEL AND SIMULATIONS

The DE method is based on the numerical solution of Newton's laws for a set of discrete, interacting particles. A recent and detailed review of this method and applications can be found in [46,47]. In our study, particles were inelastic, frictional, monodisperse spheres obeying binary, soft-sphere interactions [48] in which normal and tangential impulses are functions of a small overlap between colliding particles. Energy loss in the normal direction (i.e., along center line of contacting spheres) is produced by linear loading (K_1) and unloading springs (K_2), corresponding to a constant restitution coefficient $e=\sqrt{K_1/K_2}$. This model has been shown to reproduce the nearly linear loading behavior for a spherical surface that experiences plastic deformation of the order of 1% of a particle diameter. In the tangential direction, a Mindlin-Deresiewicz-like model [49] is used in which tangential stiffness, given by $K_T=\{\begin{smallmatrix} K_o[1-(T-\hat{T})/\mu N-\hat{T}]^{1/3}, & \textit{increasing } T \\ K_o[1-(\hat{T}-T)/\mu N+\hat{T}]^{1/3}, & \textit{decreasing } T \end{smallmatrix}\}$, (where $K_o=0.8K_1$), decreases with tangential displacement until full sliding occurs at the friction limit μ [50]. Here, $\hat{T}$ is initially equal to zero; subsequently, it is set to the value of the total tangential force when the tangential displacement changes direction.

The computational domain is again a laterally periodic box $(12d \times 12d)$ in which particles randomly placed at $t=0$ within the box are allowed to settle under gravity to a fill height of approximately 22 particle diameters. We note that the number of spheres in these studies was the same as for the MC simulations. By tuning the value of the friction coefficient μ, it is possible to obtain a wide range of solids fractions. This is demonstrated in the simulation results summarized in Fig. 7, which were obtained by averaging twenty independent realizations of poured particles. For large friction coefficients, less dense systems are produced after pouring due to the formation of bridges and arches within the structure [51–53]. For smooth particles $(\mu=0)$, the bulk solids fractions obtained are in good agreement with the value (0.6366 ± 0.0005) normally attributed to a random packing of spheres [54]. We note that the dependence of the solids fraction on friction coefficient has been reported for spheres [55] and for disks [36].

For the remainder of the discussion, we restrict attention to spheres for which $e=0.9$, $\mu=0.1$, and $\rho=1200$ kg/m^3. These properties are close to those measured by Louge [56] for acrylic spheres (i.e., $\mu=0.096 \pm 0.006$ and $e=0.934 \pm 0.009$). It is understood that these material properties may also have significant influence on system behavior. A detailed study of these effects will be the subject of future work.

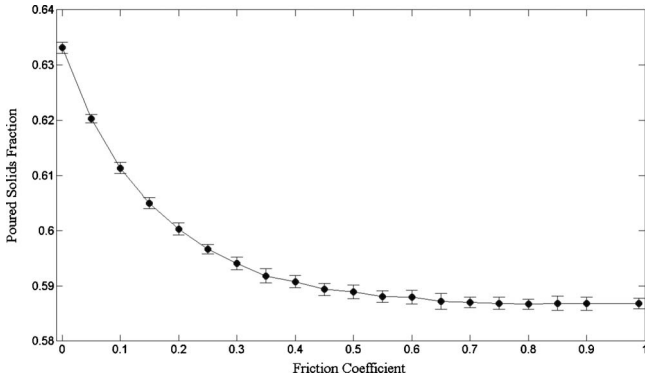

FIG. 7. A wide range of bulk densities can be obtained by changing particle friction properties. Each point on the graph represents an average taken over 20 discrete element realizations with the vertical lines representing the deviation from the average.

A. Ensemble-average bulk density evolution

We find that for poured configurations which are statistically indistinguishable with respect to their initial bulk solids fractions and distributions of nearest neighbors and free volume, significant variations in the solids fraction evolutions were observed. This is not surprising since intuition suggests that the details of the microstructure have a dominant influence on how the system advances to a dense configuration. We demonstrate this with an ensemble of 20 poured realizations with bulk solids fractions in the range 0.6088 ± 0.0035.

For each realization, the Voronoi diagram was constructed, from which the distribution of nearest neighbors (i.e., coordination number distribution) was obtained. The distributions for all realizations were individually fit $(R^2 \geq 0.9906)$ to a normal form $f(n)=\frac{1}{b\sqrt{2\pi}}\exp[-\frac{(n-a)^2}{2b^2}]$, and the fit parameters of a and b were found for each realization. The mean and standard deviation for these parameters was $a=7.2713 \pm 0.0558$ and $b=1.2550 \pm 0.0262$. Although not shown here, each of these individual distributions was statistically indistinguishable from the coordination number distribution computed from the ensemble average of the distributions ($R^2=0.9975$, $a=7.271$, and $b=1.256$). Figure 8 shows this ensemble average coordination number as well as the normal fit to this data. Another measure of the microstructure is the free volume, defined here as the difference between the volumes of the polyhedron and the encapsulated sphere. Although not shown in this paper, we also observed very little visual difference between the free volume distributions of the ensemble of 20 realizations, which were quite similar (both qualitatively and quantitatively) to the ensemble-averaged distribution given in Fig. 9.

Thus, from the perspective of bulk density, coordination number, and free volume distribution, each realization in the ensemble was very similar. And yet, the bulk solids fraction

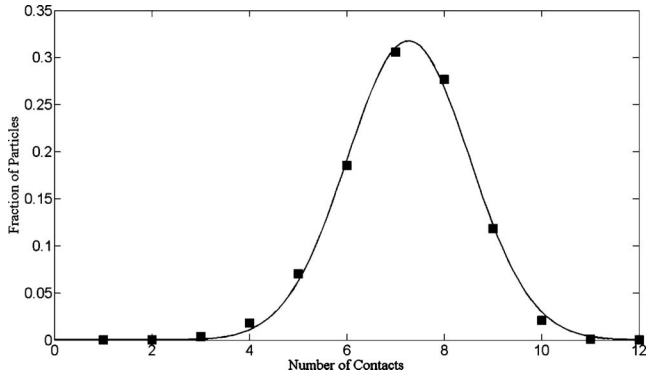

FIG. 8. The points are ensemble-averaged coordination numbers for 20 poured realizations. The solid line is a fit ($R^2=0.9975$) to $f(n)=\frac{1}{b\sqrt{2\pi}}\exp[-\frac{(n-a)^2}{2b^2}]$, where $a=7.271$ and $b=1.256$.

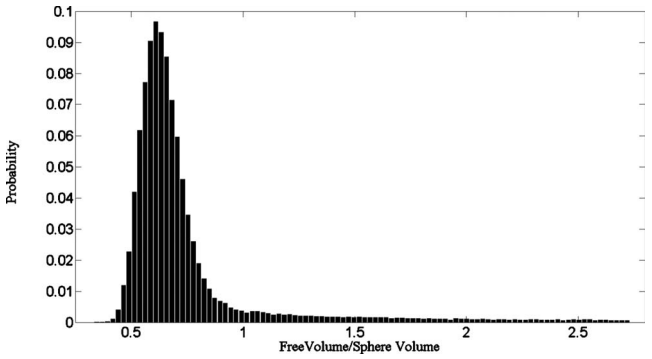

FIG. 9. Ensemble-averaged free volume (normalized by the volume of the spherical particle) distribution for 20 poured discrete element realizations.

trajectories of the realizations (obtained by tapping the poured configurations) were rather different. Taps were produced by applying harmonic displacement oscillations to the floor, consisting of a half-sine wave (amplitude α and period τ), followed by a relaxation time t_r of sufficient duration to ensure that upon collapse a quiescent state of minimal kinetic energy was attained. Each poured realization was tapped for the same time duration using identical vibration parameters, i.e., $a/d=0.4413$ and $f=7.5$ Hz, corresponding to $\Gamma=2$. The ensemble-averaged trajectory of the bulk solids fraction (for which $\langle\nu\rangle|_{t=680}=0.6997\pm0.0058$) is given in Fig. 10(a), where the inset shows the standard deviation. In some of the trajectories, rather dramatic jumps or steep gradients in the solids fraction [see Fig. 10(b)] occurred, which at first glance appeared to be spurious. However, further consideration of these trajectories suggested that the jumps were caused by collective reorganizations of the microstructure that took place over small time durations relative to the time of tapping. The later study demonstrates the sensitive dependence of the trajectories on the details of the microstructure, and the importance of using ensemble averages (rather than only single realizations) in these simulations to obtain statistically meaningful evolution curves. We do expect (in agreement with [57,58]) that the equilibrium or final solids fraction of the assembly is not consequent on the initial microstructure. However, the tap parameters do have a significant effect on the final state as will be shown in the next section.

B. Dependence on tap amplitude and frequency

The occurrence of densification strongly depends on the choice of the tap amplitude; the plot in Fig. 11 demonstrates the striking difference between the evolution of bulk solids fraction for $\Gamma=0.5$ ($f=7.5$ Hz and $a/d=0.1103$) and $\Gamma=2.0$ ($f=7.5$ Hz and $a/d=0.4413$). This is further illustrated in Fig. 12, which shows the dependence (as a function of y/d) of the solids fraction at several tap numbers for the two cases of Fig. 11. The qualitative behavior of $\bar{n}$ (the number of sphere centers at a given position y/d from the floor) at $\Gamma=2.0$ shown in Fig. 13 is comparable to the MC results (Fig. 6); that is, as the taps progress, one observes that the density increases starting from the floor. Moreover, after application of hundreds of taps, the effective height of the system is reduced by approximately two particle diameters (analogous to what took place in the MC simulations). We note that formation of ordered structures in shaken granular system was discussed in some detail recently [45], although in that work the authors have found that more complicated horizontal or horizontal/vertical vibrations were required in order to produce order. Instead, here we concentrate here on influence of the parameters governing the vibrations, as discussed in what follows.

In order to further illustrate the influence of a reduced amplitude (at constant frequency) on the development of ordered layers and the eventual increase in bulk density of the system with increasing number of taps, we carefully monitored the evolution of particle centers as a function of distance y/d from the floor for the two example cases already discussed, i.e., $f=7.5$ Hz, $a/d=0.1103$, and $\Gamma=0.5$ and $f=7.5$ Hz, $a/d=0.4413$, and $\Gamma=2.0$. This evolution for the case $\Gamma=2.0$ is presented in Fig. 14, where the vertical axis ($\bar{n}$) represents the ensemble-averaged (over 20 realizations) number of particle centers (normalized by the number of particles in the system) as a function of the position above the floor. (Note that Fig. 13 are slices taken from Fig. 14 at discrete times.) We observed that as the number of taps grew, there was an increase in the number of layers (starting from the floor) in which the location of the peaks closely corresponded with those for a hexagonal close-packed structure. Figure 14 shows the structural evolution, where $\langle\nu\rangle\approx0.7$ upon completion of 898 taps. However, for the case with the smaller amplitude ($a/d=0.1101$) no definitive organization was present upon completion of thousands of taps. This behavior supports the finding in the MC simulations of a critical value of the tap amplitude that optimizes the formation of an ordered microstructure. Within the context of the DE simulations, we interpret this amplitude as being related to a peak dilation of the system. Indeed, one can imagine two extremes that engender no microstructure development or appreciable increase in bulk density: (i) an aggressive energetic tap that greatly expands the system so that any existing microstructure is destroyed upon contraction and (ii) a low-energy tap that merely transmits a stress wave through the contact network, but does not dislodge or disturb the structure to any appreciable degree. Thus, we hypothesize that the

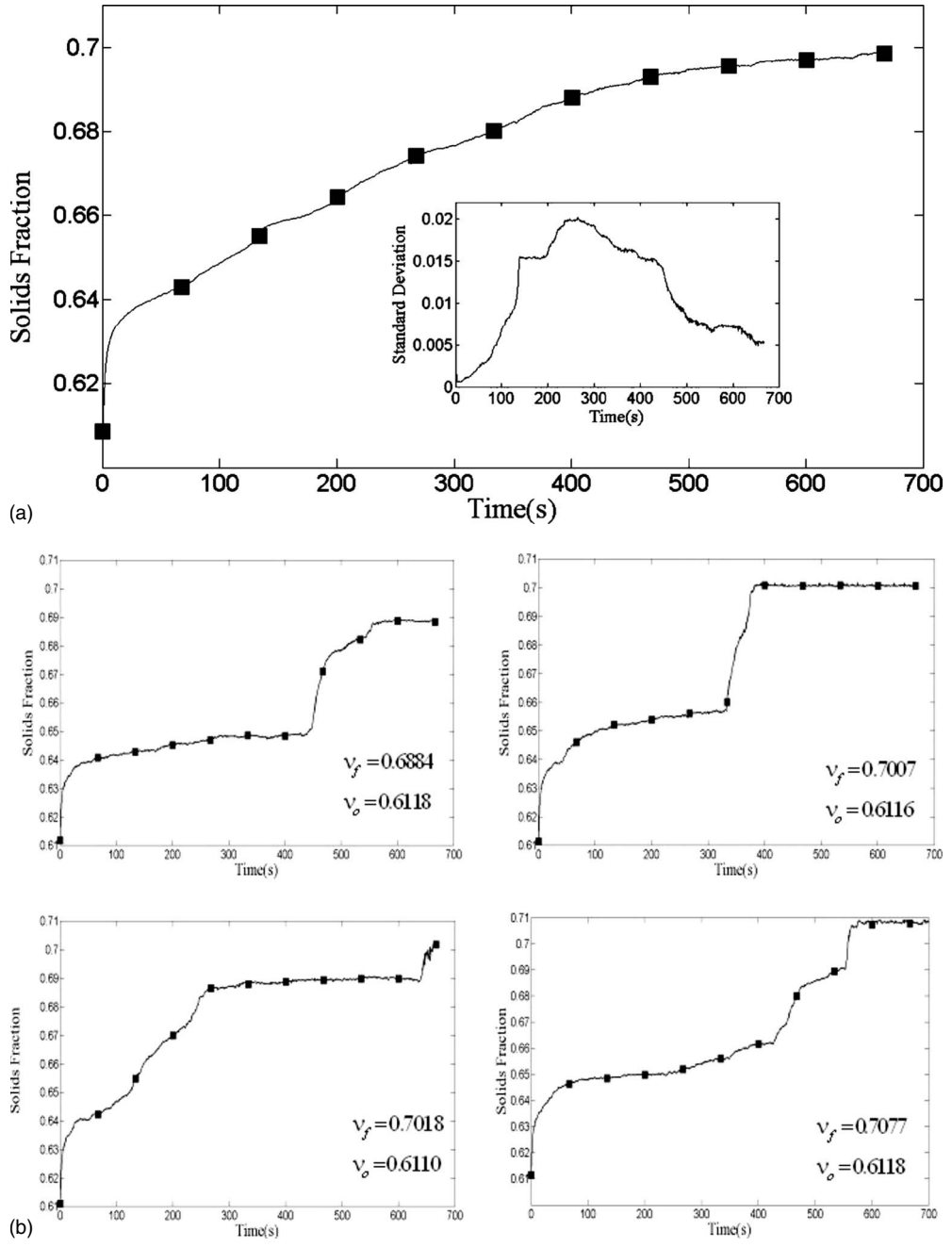

FIG. 10. (a) Evolution of the ensemble-averaged bulk solids fraction over 20 discrete element simulations in which $f=7.5$ Hz, $a/d=0.4413$, and $\Gamma=2$. The inset shows the standard deviation. (b) Several trajectories from the ensemble of 20 realizations.

densification process is regulated by the degree of dilation, and that ordering of the microstructure occurs within some narrow range of values of dilatations. The results of a study to explore this conjecture will be reported in a future paper.

Of particular relevance to the results described here are the studies of Zhu *et al.* [45], who report on experiments and discrete element simulations of the density relaxation process through the application of continuous vibrations. In particular, those authors employ a procedure in which very dense structures (solids fraction ~0.7 and higher) are built up by vibrating sequentially deposited thin poured layers (of approximately one diameter). This procedure differs from our approach, in which the entire system is exposed to taps, resulting in its evolution to a dense structure ($\langle\nu\rangle\sim0.7$) as in Fig. 10(a). Their findings are essentially in agreement with our earlier reported discrete element investigation [37] in that high solids fractions (greater than ~0.66) were not found in relatively deep systems through the application of continuous vibrations. This can be seen in the phase portrait of Fig. 15 (redrawn from [37]) for a DE simulated system of 8 000 particles ($e=0.9$ and $\mu=0.1$) within a laterally periodic box (aspect ratio $L/d=25$), in which the improvement in solids fraction $(\nu_\infty-\nu_o)/\nu_o$ is mapped as a function of the vibration amplitude ($0.02\leq a.d\leq0.48$) and frequency ($10\leq f\leq90$ Hz). Distinct regions are visible according to the color scale corresponding to various improvement levels,

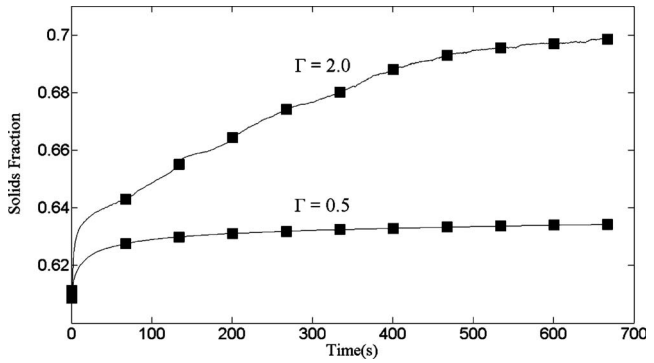

FIG. 11. Evolution of the ensemble-averaged bulk solids fraction from the discrete element simulations (over 20 realizations) for $\Gamma=0.5$ ($f=7.5$ Hz, $a/d=0.1103$) and $\Gamma=2$ ($f=7.5$ Hz, $a/d=0.4413$).

with a maximum value of only approximately 5%. Although not shown here, results from this study also indicated that these regions are correlated with depth profiles of granular temperature, solids fraction and the ratio of the lateral to vertical components of the kinetic energy. Figure 15 may represent a typical phase portrait associated with the density relaxation process, albeit quantitative differences are expected based on the mode of energy input (tapping as opposed to continuous vibrations), and on material properties, aspect ratios and mass overburdens. The result of our current exploration of the phase diagram associated with tapping dynamics will be reported in a subsequent paper.

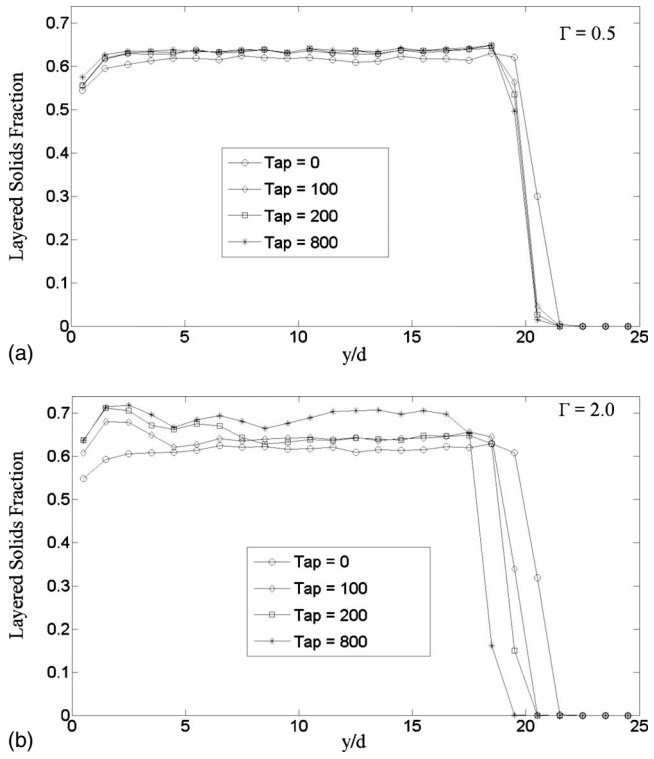

FIG. 12. Ensemble-averaged solids fraction as a function of y/d for the initial configuration, and at tap numbers 100, 200 and 800 for (a) $\Gamma=0.5$ ($f=7.5$ Hz, $a/d=0.1103$) and (b) $\Gamma=2$ ($f=7.5$ Hz, $a/d=0.4413$).

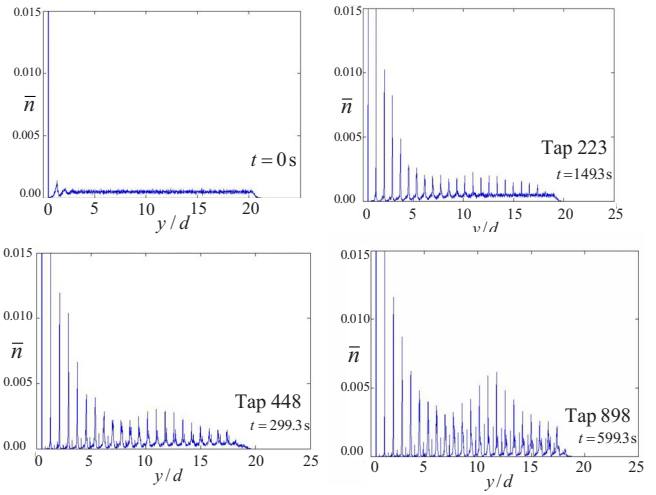

FIG. 13. (Color online) Ensemble-averaged (over 20 realizations) distributions of the particle centers measured from the floor ($y/d=0$) to the top surface for $a/d=0.4413$, $f=7.5$ Hz ($\Gamma=2.0$) at $t=0$, 149.3, 299.3, and 599.3 s.

IV. SUMMARY AND CONCLUSIONS

In this paper, the results of our MC and DE investigations of tapped density relaxation were reported. Good agreement of the MC-generated coordination number versus solids fraction with reported experiments was found. We find compelling evidence of a critical tap intensity that optimizes the evolution of packing density. Both our stochastic (MC) and deterministic (DE) models revealed the same dynamical process responsible for density relaxation, namely, the progression of self-organized layers induced by the plane floor as the taps evolve. Furthermore, our results suggest that the evolution of bulk density is highly dependent on the microstructure and contact network. We expect that this prediction will

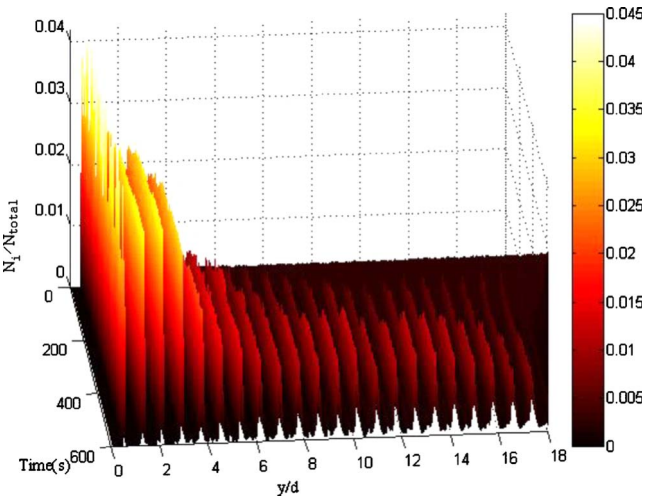

FIG. 14. (Color online) Evolution of the ensemble-averaged distribution of particle centers for $\Gamma=2$ ($f=7.5$ Hz, $a/d=0.4413$).

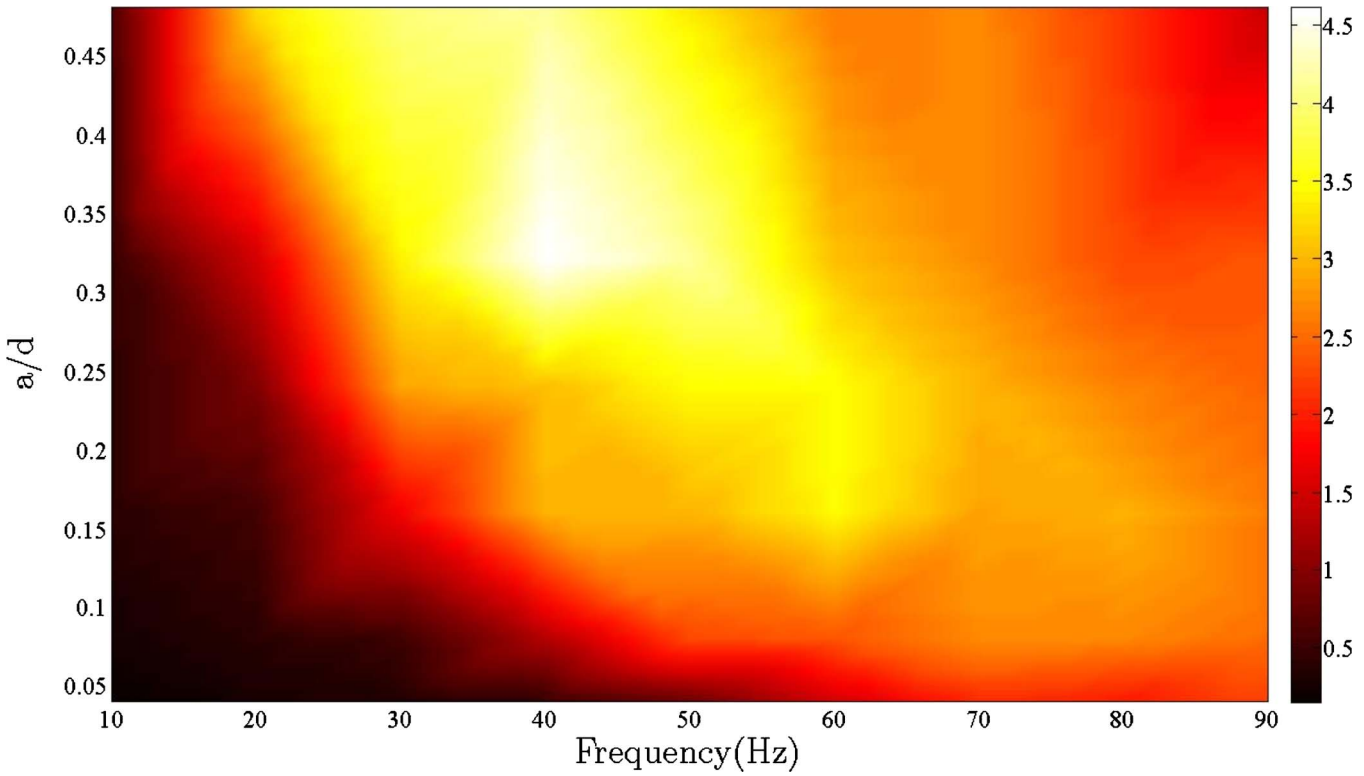

FIG. 15. (Color online) The color scale shows the improvement in bulk solids fraction $(\nu_\infty - \nu_o)/\nu_o$ as a function of amplitude ($0.02 \leq a/d \leq 0.48$) and frequency ($10\ \text{Hz} \leq f \leq 90\ \text{Hz}$) for continuously sinusoidal vibrations applied the floor (taken from [37]).

be of interest to numerous scientific and engineering problems involving self-organization and its relation to the approach to equilibrium. In future work, we will carry out a broad systematic DE study of dilation behavior and its relationship to the relaxed state, including the dependence of the relaxation process on material parameters.

ACKNOWLEDGMENTS

The authors thank D. Blackmore, P. Singh and J. T. Jenkins (Cornell University) for discussions of this work, and T. Duong who wrote the code to generate the Voronoi constructions. D.J.H. acknowledges partial support from the Grant No. NSF-DMS-0406633 and L.K. from the Grants No. NSF-DMS-0605857 and No. NSF-DMS-0835611. Partial computational support was provided by Grant No. NSF-DMS-0420590. In addition, a portion of this research was done using resources of the Open Science Grid, which is supported by the National Science Foundation and the U.S. Department of Energy's Office of Science.

[1] D. J. Cumberland and R. J. Crawford, *The Packing of Particles* (Elsevier, New York, 1987), Vol. 6.
[2] J. E. Ayer and F. E. Soppet, J. Am. Ceram. Soc. **48**, 180 (1965).
[3] P. E. Evans and R. S. Millman, Powder Metall. **7**, 50 (1964).
[4] M. Takahashi and S. Suzuki, Ceram. Bull. **65**, 1587 (1986).
[5] J. B. Knight, C. G. Fandrich, C. N. Lau, H. M. Jaeger, and S. R. Nagel, Phys. Rev. E **51**, 3957 (1995).
[6] E. R. Nowak, A. Grushin, A. C. B. Barnum, and M. B. Weissman, Phys. Rev. E **63**, 020301(R) (2001).
[7] E. R. Nowak, J. B. Knight, E. Ben-Naim, H. M. Jaeger, and S. R. Nagel, Phys. Rev. E **57**, 1971 (1998).
[8] E. R. Nowak *et al.*, Powder Technol. **94**, 79 (1997).
[9] T. Boutreux and P. G. DeGennes, Physica A **244**, 59 (1997).
[10] K. L. Gavrilov, Phys. Rev. E **58**, 2107 (1998).
[11] A. J. Kolan, E. R. Nowak, and A. V. Tkachenko, Phys. Rev. E **59**, 3094 (1999).
[12] J. Talbot, G. Tarjus, and P. Viot, Eur. Phys. J. E **5**, 445 (2001).
[13] M. Wackenhut and H. J. Herrmann, Phys. Rev. E **68**, 041303 (2003).
[14] S. J. Linz, Phys. Rev. E **54**, 2925 (1996).
[15] S. J. Linz and A. Dohle, Phys. Rev. E **60**, 5737 (1999).
[16] D. Arsenovic, S. B. Vrhovac, Z. M. Jaksic, L. Budinski-Petkovic, and A. Belic, Phys. Rev. E **74**, 061302 (2006).
[17] G. C. Barker and A. Mehta, Phys. Rev. A **45**, 3435 (1992).
[18] G. Liu and K. E. Thompson, Powder Technol. **113**, 185 (2000).
[19] L. F. Liu, Z. P. Zhang, and A. B. Yu, Physica A **268**, 433 (1999).
[20] M. Nicodemi and A. Coniglio, Phys. Rev. Lett. **82**, 916

(1999).
[21] M. Nicodemi, A. Coniglio, and H. J. Herrmann, Phys. Rev. E **59**, 6830 (1999).
[22] S. Remond and J. L. Galias, Physica A **369**, 545 (2006).
[23] L. A. Pugnaloni, M. Mizrahi, C. M. Carlevaro, and F. Vericat, Phys. Rev. E **78**, 051305 (2008).
[24] X. Z. An, R. Y. Yang, K. J. Dong, R. P. Zou, and A. B. Yu, Phys. Rev. Lett. **95**, 205502 (2005).
[25] A. V. Anikeenko, N. N. Medvedev, and T. Aste, Phys. Rev. E **77**, 031101 (2008).
[26] K. E. Daniels and R. P. Behringer, Phys. Rev. Lett. **94**, 168001 (2005).
[27] N. W. Mueggenburg, Phys. Rev. E **71**, 031301 (2005).
[28] J.-C. Tsai and J. P. Gollub, Phys. Rev. E **70**, 031303 (2004).
[29] O. Pouliquen, M. Nicolas, and P. D. Weidman, Phys. Rev. Lett. **79**, 3640 (1997).
[30] O. Carvente and J. C. Ruiz-Suarez, Phys. Rev. Lett. **95**, 018001 (2005).
[31] O. Carvente and J. C. Ruiz-Suarez, Phys. Rev. E **78**, 011302 (2008).
[32] M. Nakagawa and S. Luding, *Proceedings of the 6th International Conference on Micromechanics of Granular Media* (AIP, Melville, NY, 2009), Vol. 1145.
[33] O. Dybenko, A. D. Rosato, and D. Horntrop, Kona **25**, 133 (2007).
[34] N. Metropolis *et al.*, J. Chem. Phys. **21**, 1087 (1953).
[35] S. Luding, M. Nicolas, and O. Pouliquen, e-print arXiv:cond-mat/0003172.
[36] M. P. Ciamarra and A. Coniglio, Phys. Rev. Lett. **101**, 128001 (2008).
[37] N. Zhang and A. D. Rosato, Kona **24**, 93 (2006).
[38] P. Ribiere, P. Richard, R. Delannay, D. Bideau, M. Toiya, and W. Losert, Phys. Rev. Lett. **95**, 268001 (2005).
[39] T. Aste, M. Saadatfar, and T. J. Senden, Phys. Rev. E **71**, 061302 (2005).
[40] P. Philippe and D. Bideau, Europhys. Lett. **60**, 677 (2002).
[41] J. C. Macrae, W. A. Gray, and P. C. Finlason, Nature (London) **179**, 1365 (1957).
[42] E. M. Kelly, Powder Technol. **4**, 56 (1970).
[43] T. G. Owe Berg, R. L. McDonald, and R. J. Trainor, Powder Technol. **3**, 183 (1969).
[44] P. Philippe, Ph. D. dissertation, University of Rennes I, Rennes, France, 2002.
[45] A. B. Yu, X. Z. An, R. P. Zou, R. Y. Yang, and K. Kendall, Phys. Rev. Lett. **97**, 265501 (2006).
[46] H. P. Zhu, Z. Y. Zhou, R. Y. Yang, and A. B. Yu, Chem. Eng. Sci. **62**, 3378 (2007).
[47] H. P. Zhu, Z. Y. Zhou, R. Y. Yang, and A. B. Yu, Chem. Eng. Sci. **63**, 5728 (2008).
[48] O. R. Walton and R. L. Braun, Acta Mech. **63**, 73 (1986).
[49] R. D. Mindlin and H. Deresiewicz, ASME J. Appl. Mech. **20**, 327 (1953).
[50] O. R. Walton, Mech. Mater. **16**, 239 (1993).
[51] L. A. Pugnaloni, G. C. Barker, and A. Mehta, Adv. Complex Syst. **4**, 289 (2001).
[52] L. A. Pugnaloni and G. C. Barker, Physica A **337**, 428 (2004).
[53] G. C. Barker, in *The Chemical Physics of Food*, edited by P. Belton (Blackwell, Oxford, 2007), p. 135.
[54] G. D. Scott and D. M. Kilgour, Br. J. Appl. Phys. **2**, 863 (1969).
[55] L. E. Silbert, D. Ertas, G. S. Grest, T. C. Halsey, and D. Levine, Phys. Rev. E **65**, 031304 (2002).
[56] M. Y. Louge, http://www.mae.cornell.edu/microgravity/impact-table.html.
[57] M. Pica Ciamarra, A. Coniglio, and M. Nicodemi, Phys. Rev. Lett. **97**, 158001 (2006).
[58] P. Ribiere *et al.*, Eur. Phys. J. E **22**, 249 (2007).